VIP Retinal Regeneration Very Important Paper

Deutsche Ausgabe: DOI: 10.1002/ange.201505798
Internationale Ausgabe: DOI: 10.1002/anie.201505798

Influence of Arrestin on the Photodecay of Bovine Rhodopsin

Deep Chatterjee, Carl Elias Eckert, Chavdar Slavov, Krishna Saxena, Boris Fürtig, Charles R. Sanders, Vsevolod V. Gurevich, Josef Wachtveitl, and Harald Schwalbe**

Abstract: *Continued activation of the photocycle of the dim-light receptor rhodopsin leads to the accumulation of all-trans-retinal in the rod outer segments (ROS). This accumulation can damage the photoreceptor cell. For retinal homeostasis, deactivation processes are initiated in which the release of retinal is delayed. One of these processes involves the binding of arrestin to rhodopsin. Here, the interaction of pre-activated truncated bovine visual arrestin (Arr^{Tr}) with rhodopsin in 1,2-diheptanoyl-sn-glycero-3-phosphocholine (DHPC) micelles is investigated by solution NMR techniques and flash photolysis spectroscopy. Our results show that formation of the rhodopsin–arrestin complex markedly influences partitioning in the decay kinetics of rhodopsin, which involves the simultaneous formation of a meta II and a meta III state from the meta I state. Binding of Arr^{Tr} leads to an increase in the population of the meta III state and consequently to an approximately twofold slower release of all-trans-retinal from rhodopsin.*

The mammalian visual cycle is a complex process involving activation, deactivation, and regeneration pathways.[1–6] The prototype G-protein-coupled receptor (GPCR) rhodopsin plays a pivotal role in this system. The extensive study of this system has provided much information that is believed to generally apply to the signaling pathways of other GPCRs.[7–9] One of the breakthroughs in rhodopsin and GPCR research was the elucidation of the crystal structure of bovine rhodopsin,[10] which provided a platform for future structural and functional studies on GPCRs.[7–9]

[*] D. Chatterjee,[+] Dr. K. Saxena, Dr. B. Fürtig, Prof. Dr. H. Schwalbe
Institute of Organic Chemistry and Chemical Biology
Center of Biomolecular Magnetic Resonance (BMRZ)
Goethe University Frankfurt/Main
Max-von-Laue-Strasse 7, 60438 Frankfurt am Main (Germany)
E-mail: schwalbe@nmr.uni-frankfurt.de

C. E. Eckert,[+] Dr. C. Slavov, Prof. Dr. J. Wachtveitl
Institute of Physical and Theoretical Chemistry
Goethe University Frankfurt/Main
Max-von-Laue-Strasse 7, 60438 Frankfurt am Main (Germany)
E-mail: wveitl@theochem.uni-frankfurt.de

Prof. Dr. C. R. Sanders
Department of Biochemistry, Center for Structural Biology, Institute of Chemical Biology, Vanderbilt University School of Medicine
Nashville, TN 37232 (USA)

Prof. Dr. V. V. Gurevich
Department of Pharmacology
Vanderbilt University School of Medicine
Nashville, TN 37232 (USA)

[+] These authors contributed equally to this work.

Supporting information for this article is available on the WWW under http://dx.doi.org/10.1002/anie.201505798.

Rhodopsin adopts a seven transmembrane α-helical structure and carries the covalently attached retinal chromophore. Photoinduced isomerization of the chromophore from its 11-*cis* to all-*trans* configuration results in conformational changes in rhodopsin that lead to the formation of several transiently populated intermediate states (Figure 1).[10–16] Early photointermediates are short-lived and convert into a meta I state on a sub-millisecond time scale. This meta I state functions as a juncture at which the photocycle bifurcates to form meta II and meta III states.[17] The meta II state interacts with the guanine nucleotide binding protein (G protein) transducin and triggers the activation signaling cascade, finally leading to hyperpolarization of photoreceptor cells. The meta III state has been reported to function as an energy-storage state.[18] The distribution between states populated along the photodecay can be shifted by changing the conditions, including temperature and pH.[19–21] Both the meta II and meta III states finally relax to the apoprotein opsin through release of all-*trans*-retinal.

Prolonged exposure to light can lead to an accumulation of free all-*trans*-retinal in the rod outer segment (ROS), which can be toxic to the eye owing to the formation of epoxides by oxidation. Harmful effects of excess retinal include visual dysfunction and retinal damage as found in several diseases, such as age-related macular degeneration (AMD).[22–24] Previously published data[25,26] suggest that there are two rate-limiting steps that maintain the level of all-*trans*-retinal in the ROS: 1) the release of free all-*trans*-retinal that depends on the photodecay kinetics and 2) the conversion of retinal into retinol by the enzyme retinal dehydrogenase (RDH; Figure 1). As the rate of enzymatic turnover of RDH is slow compared to meta II decay, retinal can accumulate in the ROS.[25,27,28] When retinal accumulates, the eye initiates photocycle deactivation processes to delay the release of retinal.[29]

Visual arrestin, a protein that belongs to the arrestin subfamily, acts as the major facilitator that down-regulates rhodopsin signaling by tightly binding to rhodopsin and concomitant displacement of G protein.[30,31] A recently published crystal structure of the rhodopsin–arrestin complex has provided insights into the static nature of this interaction.[32] Arrestin binding has been shown to slow down retinal release by stabilization of the meta II state.[33] However, the effect of arrestin on the meta III photodynamics has not been studied in detail.

Aside from full-length arrestin, p44 (Arr1–370A), a splice variant of arrestin,[34] is also present in rod cells. Although p44 is not ubiquitously present among all species (for example, in mice), it has been suggested to play a role in rhodopsin deactivation.[34–37] The binding mechanism of p44 to rhodopsin is different from that of arrestin owing to the absence of the C-terminal tail.[34–37] p44 not only binds more tightly to

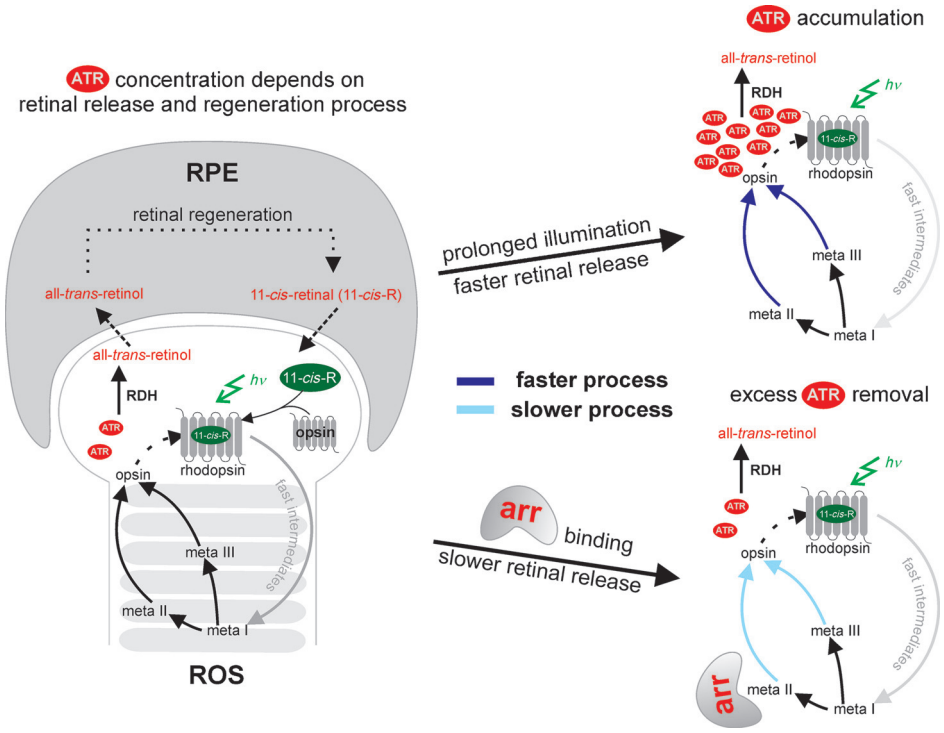

Figure 1. Mammalian visual cycle. The concentration of free all-*trans*-retinal (ATR) depends on two processes: 1) retinal release during the photocycle in the rod outer segment (ROS) and 2) retinal removal by a regeneration pathway in the retinal pigment epithelium (RPE) as shown on the left. Continuous exposure to light leads to the accumulation of ATR (top right), which initiates rhodopsin deactivation by arrestin (arr). Arrestin binding slows down the retinal release, which provides retinal dehydrogenase (RDH) with ample time to remove excess ATR by converting it into all-*trans*-retinol (bottom right).

phosphorylated rhodopsin, but also binds to the non-phosphorylated form.[36,37] Owing to the latter interaction, it has previously been argued that phosphorylation is not needed for p44-mediated rhodopsin deactivation.[34,37] However, it is not known how p44 manipulates the rhodopsin decay kinetics, especially the meta III dynamics.

Herein, we investigated the effect of p44 on the photodecay kinetics of rhodopsin. We employed a truncated mutant (Arr1–378) of visual arrestin (Arr^{Tr}),[38] which is devoid of the C-terminal tail. Arr^{Tr} closely resembles p44, including phosphorylation-independent deactivation of rhodopsin.[38] We utilized Arr^{Tr} instead of p44 as it is less prone to aggregation. To analyze the interaction, we employed a strategy combining two biophysical techniques, NMR spectroscopy and flash photolysis.

Our NMR analysis of the dynamics of photoactivated rhodopsin was based on the kinetic behavior of five tryptophan residues present in rhodopsin, which were used as reporter groups (Figure 2a). All five tryptophan indole resonances were previously assigned in *n*-dodecyl-β-D-maltoside (DDM) micelles by utilizing single-point tryptophan to phenylalanine mutants.[17] As previous studies had shown that arrestin is destabilized in the presence of DDM,[39] we utilized 1,2-diheptanoyl-*sn*-glycero-3-phosphocholine (DHPC) for the interaction studies of rhodopsin and Arr^{Tr}.[34,37] Rhodopsin is expressed in HEK293 cells;[40,41] this expression yields the non-phosphorylated form of the protein.

Initially, the differences in the ground-state structures of DDM- and DHPC-solubilized rhodopsin were characterized using 2D NMR spectroscopy, followed by an investigation of the effect of different detergents on the photodecay of rhodopsin. The chemical shift perturbations (CSPs) for the tryptophan indole resonances in DHPC micelles remain almost identical to those in DDM (Figure 2b). Hence the assignments for each of these tryptophan resonances could be easily transferred from the previous assignment in DDM. The similarity of the CSPs also indicates that the overall fold of rhodopsin is not significantly altered upon replacing the DDM with DHPC micelles.

To investigate the influence of Arr^{Tr} on the dark state of rhodopsin, we performed 2D ^{1}H, ^{15}N correlation experiments. The interaction with Arr^{Tr} induces both CSPs and the disappearance of a subset of NMR signals in the amide region of the spectra arising from residues in the flexible C-terminal part of rhodopsin (Figure 2c).[42–47] The five NMR resonances of the tryptophan indole sidechains (Figure 2d), however, are not altered, indicating that low-affinity transient binding of Arr^{Tr} to rhodopsin in the dark does not lead to a major structural rearrangement in the transmembrane helical part.[37,39]

Our previous results on the kinetic analysis of rhodopsin in DDM micelles showed complex photodecay kinetics with two different rate constants detected for different tryptophan reporter groups and a third, substantially slower decay constant owing to protein aggregation.[17] In DDM, W126, W161, and W265 formed a first group of residues with a common lifetime of 8 min (t_1). The second process, which could be observed for W35 and W175, had a lifetime of 34 min (t_2). We previously proposed that these two lifetimes represent decay by a direct route involving meta II and by a branched route populating an alternative-pathway meta III state, respectively.[17]

Time-resolved NMR experiments of the rhodopsin kinetics in a DHPC micelle (Figure 3a) revealed faster decay of the five tryptophan resonances than in a DDM micelle. A lower signal-to-noise ratio and the significantly faster decay in DHPC made the analysis of the NMR-derived kinetic data more difficult. Therefore, we focused on the kinetic analysis of the two most intense indole signals, W126 and W35 (Figure 3b). W126 showed a decay time of 5 min, whereas W35 showed a decay time of 7 min (Table 1). Similar to our previous kinetic analysis in DDM, the presence of two

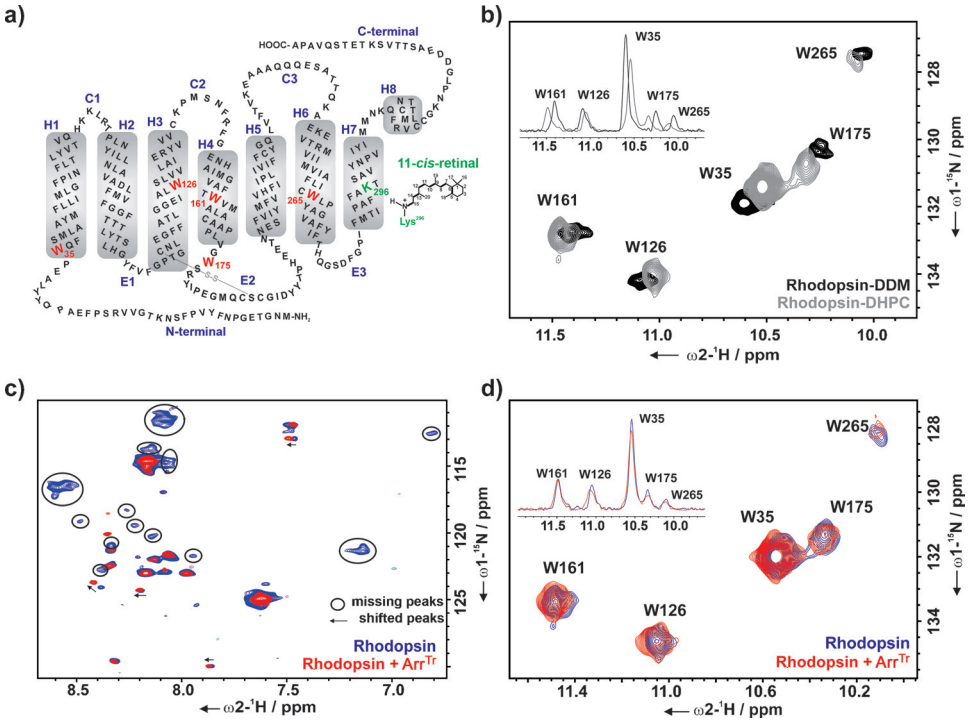

Figure 2. a) Secondary structure of bovine rhodopsin with the five tryptophan residues (W35, W126, W161, W175, and W265) used as reporter groups in the NMR experiments. b) Overlay of the indole region of 2D ^{1}H, ^{15}N SOFAST-HMQC spectra of α,ε-^{15}N-tryptophan-labeled rhodopsin in DDM (black) and DHPC (gray) micelles. c,d) Overlays of the 2D ^{1}H, ^{15}N SOFAST-HMQC spectra of α,ε-^{15}N-tryptophan-labeled rhodopsin without (blue) and with Arr^{Tr} (red; rhodopsin/Arr^{Tr} = 1:2) showing the backbone (c) and indole (d) regions of the spectra. Overlays of the 1D projections of the corresponding cross peaks of the indole region of the 2D spectra are shown in the insets (b and d). All spectra were recorded at 800 MHz (T = 298 K) in the following buffer solutions: DDM spectrum: 20 mM sodium phosphate buffer, pH 7.4; DHPC spectra: 25 mM Tris, pH 7.5, 100 mM NaCl, 0.1 μM EDTA, 10% D_2O, and 1 mM 3-(trimethylsilyl)-2,2′,3,3′-tetradeuteropropionic acid ([D_4]-TSP).

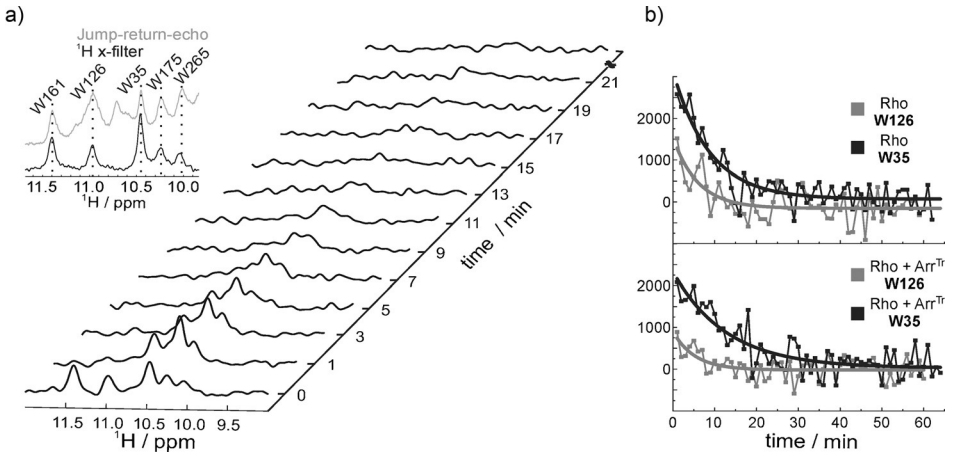

Figure 3. NMR kinetics. a) A series of 1D ^{1}H NMR spectra of α,ε-^{15}N-tryptophan-labeled rhodopsin recorded at different time intervals after illumination. The indole region of the spectrum is shown. The five resonances visible in the dark state correspond to the five tryptophan residues present in rhodopsin. After illumination, the 1D ^{1}H spectra were recorded with a temporal resolution of one minute. Inset: Overlay of the spectra of the jump–return–echo (gray) and ^{1}H x-filter (black) NMR experiments with rhodopsin samples. The dashed lines connect the corresponding resonances of the five tryptophan residues. b) Extracted signal intensities from a series of 1D ^{1}H NMR spectra of α,ε-^{15}N-tryptophan-labeled rhodopsin in the presence and absence of Arr^{Tr}. A mono-exponential fit was applied for the signal intensities of W35 (black curve) and W126 (gray curve).

lifetimes in our current data suggest that the kinetic partitioning of the photodecay, seen in DDM[17] and even in native disk,[21] was preserved in DHPC.

Upon addition of Arr^{Tr}, all five tryptophan indole resonances broadened, indicating the formation of a Arr^{Tr}–rhodopsin complex. After illumination, Arr^{Tr} binding did not change the lifetime of the W126 resonance, but it increased the lifetime of the W35 resonance by a factor of 1.6 from 7 min to 9.6 min. This result indicates that Arr^{Tr} induces a change in the decay kinetics of rhodopsin photointermediates.

To investigate these complex photodynamics in more detail, we performed broadband flash photolysis. We employed a multichannel detection system to obtain spectrally resolved transient absorption data (see the Supporting Information). We used the reported absorption maxima of the relevant intermediates of rhodopsin determined for hypotonically extracted ROS disk membranes from retina[48] as references for the assignment of the spectral signatures in our transient absorption data. The transient spectra of DHPC-solubilized rhodopsin in the absence (Figure 4a) or presence of Arr^{Tr} (Figure 4b) were mainly determined by ground state bleaching (GSB) at about 500 nm and the formation of free all-*trans*-retinal at approximately 380 nm. Double difference spectra (Figure 4c,d) were calculated by subtracting the absorption change recorded at the maximum delay time from the transient absorption data. They depicted a positive signature at 400 nm, reporting on meta II decay, and a spectrally broad positive change in the absorption at 460–560 nm, representing met-

Table 1: Lifetimes of the tryptophan resonances of rhodopsin (150 μM) in the absence (−) and presence (+) of Arr^{Tr}.

	Lifetime [min]	
	−Arr^{Tr} (0 μM)	+Arr^{Tr} (300 μM)
W35	6.92 ± 0.38	9.58 ± 1.94
W126	5.03 ± 0.40	5.23 ± 2.05

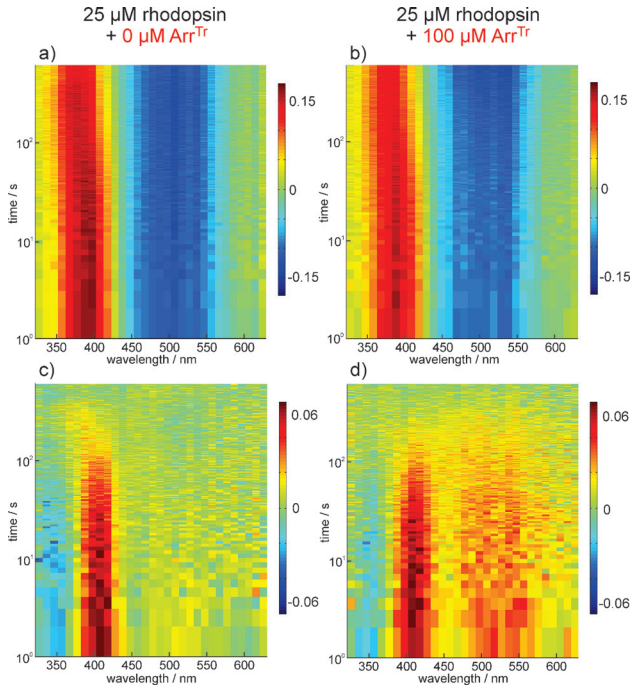

Figure 4. a, b) Transient absorption spectra of rhodopsin without (a) and with (b) Arr^{Tr}. Red and blue denote positive and negative changes in absorption, respectively. c, d) Double difference spectra of the spectra shown in (a) and (b), respectively, calculated by subtracting the absorption change recorded at the maximum delay time from the transient absorption data.

a III and potentially meta I. With Arr^{Tr}, the meta III signature was clearly more pronounced.

To visualize and quantify differences in the kinetics of these intermediates with and without Arr^{Tr}, a global lifetime analysis (GLA)[49,50] was performed on the transient absorption data $I(\lambda,t)$ (see the Supporting Information). The GLA provided the lifetimes of meta II (1–2 min) and meta III (6–7 min) decay (Figure S3) and also suggested increased meta III formation in the presence of Arr^{Tr}. The GLA lifetimes are comparable to the two lifetimes observed in the NMR kinetic analysis (Table 1).

To corroborate the GLA results, we additionally performed a lifetime density analysis (LDA).[50] With this method, the pre-exponential amplitudes of the sum of a large number (typically ca. 100) of exponential functions with fixed lifetimes (τ) are determined,

$$I(\lambda,t) = \int_0^\infty \Phi(\lambda,\tau)e^{-t/\tau}d\tau \qquad (1)$$

where τ is the time, $I(\lambda,t)$ is the normalized decay function, and $\Phi(\lambda,\tau)$ is the spectral density function. The kinetic information contained in the time-resolved data is then presented in the form of a 2D lifetime distribution map. In contrast to GLA, the LDA is model-independent and thereby also extracts non-exponential or stretched exponential kinetics.

The lifetime density maps (LDMs; Figure 5) consist of four prominent distributions, as indicated by the letters C–F, describing the photodecay dynamics (Table 2, see also the Supporting Information, Table S1). The spectral signatures A (free retinal absorption) and B (ground-state bleach) in the LDMs (Figure 5) are long-lived non-decaying components that do not describe any photodecay dynamics. Similar to the GLA results, we observed a distribution for a short lifetime describing meta II decay (C) and meta III formation (D). The distribution for the longer lifetime corresponds to meta III decay (E). We assigned signature F to the formation of free retinal. The temporal position of F indicated that retinal release proceeds through both meta II and meta III decay in the absence of Arr^{Tr}. In the presence of Arr^{Tr}, the formation of free retinal (F) was significantly delayed, which is shown by the strong shift in the lifetime of signature F from 2.5 min to

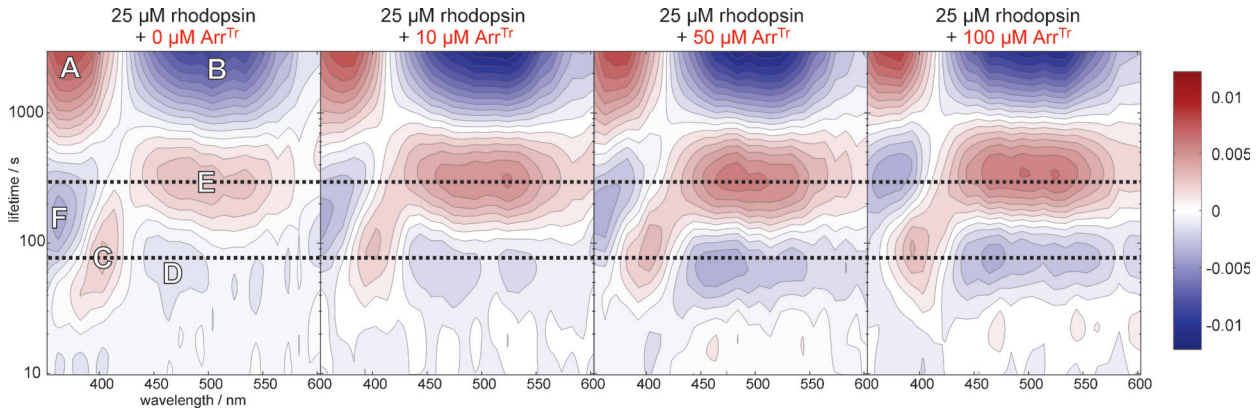

Figure 5. Lifetime density analysis of the transient absorption data. LDMs of rhodopsin samples with increasing Arr^{Tr} concentration. The reading of the LDMs is as for decay associated spectra (DAS) in GLA, with positive (red) amplitudes accounting for a decay of absorption and negative (blue) amplitudes accounting for an increase in absorption. The lifetimes and the distribution maxima of the signatures C–F are shown in Table 1.

Table 2: Lifetimes, distribution maxima, and amplitudes of the signatures C–F of the LDMs of rhodopsin (25 μM) in the absence (−) and presence (+) of Arr^{Tr}.

	Lifetime [min]		Wavelength [nm]		Amplitude	
	$-Arr^{Tr}$[e]	$+Arr^{Tr}$[f]	$-Arr^{Tr}$	$+Arr^{Tr}$	$-Arr^{Tr}$	$+Arr^{Tr}$
C[a]	1.3	1.5	400	390	0.003	0.004
D[b]	1.2	1.3	465	465	−0.001	−0.003
E[c]	5.0	5.3	460–540	460–540	0.003	0.007
F[d]	2.5	5.3	365	375	−0.004	−0.004

[a] Meta II decay. [b] Meta III formation. [c] Meta III decay. [d] Free retinal formation. [e] Arr^{Tr} concentration: 0 μM. [f] Arr^{Tr} concentration: 100 μM.

5.3 min. Moreover, the amplitudes signifying the formation (D) and decay (E) of meta III were more pronounced. From these observations, we conclude that the Arr^{Tr}–rhodopsin interaction slowed down the photodecay and thereby inhibited retinal release via meta II. As a consequence, the meta II–meta I equilibrium shifted towards meta I, which led to the accumulation of meta III. Subsequently, retinal release is delayed by a factor of two as meta III has a longer decay lifetime than meta II. A similar effect was observed in the NMR kinetic data as the decay lifetime of the W35 resonance was prolonged upon addition of Arr^{Tr} (Table 1). This effect can be attributed to a change in the protein dynamics influenced by the retinal release process.

Our findings indicate that meta III decay may have a physiological relevance on the regulation of the free all-*trans*-retinal concentration in ROS. We suggest that aside from the previously discussed rate-limiting factor for retinal regeneration within the photocycle of rhodopsin, namely the release of retinal from meta II, meta III decay can also be considered as an additional important factor for the homeostasis of the free all-*trans*-retinal concentration in ROS essential for the functionality of the eye at varying light intensities. The role of meta III, which was envisioned as an energy-storage state, as previously proposed by Bartl and Vogel[51] who stated that under "bright light and thus high bleaching conditions, a delayed release of all-*trans*-retinal during meta II decay by formation of a meta III storage might be physiologically advantageous", is fully consistent with our analysis. Here, we thus provide evidence for the function of meta III as a physiologically relevant energy-storage state.

In conclusion, this study has not only provided detailed insight into rhodopsin deactivation and the retinal regeneration process, but also pushed our time-resolved NMR and flash photolysis techniques to new limits. The data analysis was based on single-shot experiments because of the non-cyclic photodynamics of bovine rhodopsin. It required high NMR fields and advanced data analysis techniques (GLA and LDA). By using two different spectroscopic techniques, the role of arrestin in stabilizing meta III storage in the bifurcated photodecay of visual rhodopsin was unraveled at high temporal and amino acid resolution.

Acknowledgements

The work was supported by the DFG (SFB807). H.S. and J.W. are members of the DFG-funded cluster of excellence "Macromolecular Complexes". B.M.R.Z. is supported by the state of Hesse. C.R.S. and V.V.G. are supported by NIH grants (U54 GM094608 and EY011500, respectively).

Keywords: arrestin · NMR spectroscopy · retinal regeneration · rhodopsin · UV/Vis spectroscopy

How to cite: *Angew. Chem. Int. Ed.* **2015**, *54*, 13555–13560
Angew. Chem. **2015**, *127*, 13759–13764

[1] K. D. Ridge, K. Palczewski, *J. Biol. Chem.* **2007**, *282*, 9297–9301.
[2] R. O. Parker, R. K. Crouch, *Exp. Eye Res.* **2010**, *91*, 788–792.
[3] P. H. Tang, M. Kono, Y. Koutalos, Z. Ablonczy, R. K. Crouch, *Prog. Retinal Eye Res.* **2013**, *32*, 48–63.
[4] D. A. Baylor, M. E. Burns, *Eye (Lond).* **1998**, *12*, 521–525.
[5] X. E. Zhou, K. Melcher, H. E. Xu, *Acta Pharmacol. Sin.* **2012**, *33*, 291–299.
[6] V. Y. Arshavsky, T. D. Lamb, E. N. Pugh, *Annu. Rev. Physiol.* **2002**, *64*, 153–187.
[7] X. Deupi, *Biochim. Biophys. Acta Bioenerg.* **2014**, *1837*, 674–682.
[8] O. P. Ernst, D. T. Lodowski, M. Elstner, P. Hegemann, L. S. Brown, H. Kandori, *Chem. Rev.* **2014**, *114*, 126–163.
[9] S. Wolf, S. Grünewald, *PLoS One* **2015**, *10*, e0123533.
[10] K. Palczewski et al., *Science* **2000**, *289*, 739–745.
[11] H. Nakamichi, T. Okada, *Angew. Chem. Int. Ed.* **2006**, *45*, 4270–4273; *Angew. Chem.* **2006**, *118*, 4376–4379.
[12] H.-W. Choe, Y. J. Kim, J. H. Park, T. Morizumi, E. F. Pai, N. Krauss, K. P. Hofmann, P. Scheerer, O. P. Ernst, *Nature* **2011**, *471*, 651–655.
[13] P. Scheerer, J. H. Park, P. W. Hildebrand, Y. J. Kim, N. Krauss, H.-W. Choe, K. P. Hofmann, O. P. Ernst, *Nature* **2008**, *455*, 497–502.
[14] C. Altenbach, A. K. Kusnetzow, O. P. Ernst, K. P. Hofmann, W. L. Hubbell, *Proc. Natl. Acad. Sci. USA* **2008**, *105*, 7439–7444.
[15] T. D. Dunham, D. L. Farrens, *J. Biol. Chem.* **1999**, *274*, 1683–1690.
[16] H. Nakamichi, T. Okada, *Proc. Natl. Acad. Sci. USA* **2006**, *103*, 12729–12734.
[17] J. Stehle, R. Silvers, K. Werner, D. Chatterjee, S. Gande, F. Scholz, A. Dutta, J. Wachtveitl, J. Klein-Seetharaman, H. Schwalbe, *Angew. Chem. Int. Ed.* **2014**, *53*, 2078–2084; *Angew. Chem.* **2014**, *126*, 2110–2116.
[18] E. Ritter, M. Elgeti, F. J. Bartl, *Photochem. Photobiol.* **2008**, *84*, 911–920.
[19] R. G. Matthews, R. Hubbard, P. K. Brown, G. Wald, *J. Gen. Physiol.* **1963**, *47*, 215–240.
[20] K. Zimmermann, E. Ritter, F. J. Bartl, K. P. Hofmann, M. Heck, *J. Biol. Chem.* **2004**, *279*, 48112–48119.
[21] R. Vogel, F. Siebert, X. Y. Zhang, G. Fan, M. Sheves, *Biochemistry* **2004**, *43*, 9457–9466.
[22] R. A. Radu, N. L. Mata, A. Bagla, G. H. Travis, *Proc. Natl. Acad. Sci. USA* **2004**, *101*, 5928–5933.
[23] J. R. Sparrow, N. Fishkin, J. Zhou, B. Cai, Y. P. Jang, S. Krane, Y. Itagaki, K. Nakanishi, *Vision Res.* **2003**, *43*, 2983–2990.
[24] A. Wenzel, C. Grimm, M. Samardzija, C. E. Remé, *Prog. Retinal Eye Res.* **2005**, *24*, 275–306.
[25] C. Chen, E. Tsina, M. C. Cornwall, R. K. Crouch, S. Vijayaraghavan, Y. Koutalos, *Biophys. J.* **2005**, *88*, 2278–2287.
[26] M. E. Sommer, W. C. Smith, D. L. Farrens, *J. Biol. Chem.* **2005**, *280*, 6861–6871.

[27] K. Palczewski, J. P. Van Hooser, G. G. Garwin, J. Chen, G. I. Liou, J. C. Saari, *Biochemistry* **1999**, *38*, 12012 – 12019.
[28] K. P. Hofmann, A. Pulvermüller, J. Buczyłko, P. Van Hooser, K. Palczewski, *J. Biol. Chem.* **1992**, *267*, 15701 – 15706.
[29] M. E. Sommer, K. P. Hofmann, M. Heck, *Nat. Commun.* **2012**, *3*, 1 – 10.
[30] J. A. Hirsch, C. Schubert, V. V. Gurevich, P. B. Sigler, *Cell* **1999**, *97*, 257 – 269.
[31] J. Granzin, U. Wilden, H. W. Choe, J. Labahn, B. Krafft, G. Büldt, *Nature* **1998**, *391*, 918 – 921.
[32] Y. Kang et al., *Nature* **2015**, *523*, 561 – 567.
[33] M. E. Sommer, D. L. Farrens, *Vision Res.* **2006**, *46*, 4532 – 4546.
[34] W. C. Smith, A. H. Milam, D. Dugger, A. Arendt, P. A. Hargrave, K. Palczewski, *J. Biol. Chem.* **1994**, *269*, 15407 – 15410.
[35] J. Granzin, A. Cousin, M. Weirauch, R. Schlesinger, G. Büldt, R. Batra-Safferling, *J. Mol. Biol.* **2012**, *416*, 611 – 618.
[36] Y. J. Kim, K. P. Hofmann, O. P. Ernst, P. Scheerer, H.-W. Choe, M. E. Sommer, *Nature* **2013**, *497*, 142 – 146.
[37] K. Schröder, A. Pulvermüller, K. P. Hofmann, *J. Biol. Chem.* **2002**, *277*, 43987 – 43996.
[38] V. V. Gurevich, *J. Biol. Chem.* **1998**, *273*, 15501 – 15506.
[39] T. Zhuang, Q. Chen, M.-K. Cho, S. A. Vishnivetskiy, T. M. Iverson, V. V. Gurevich, C. R. Sanders, *Proc. Natl. Acad. Sci. USA* **2013**, *110*, 942 – 947.
[40] P. J. Reeves, J.-M. Kim, H. G. Khorana, *Proc. Natl. Acad. Sci. USA* **2002**, *99*, 13413 – 13418.
[41] P. J. Reeves, N. Callewaert, R. Contreras, H. G. Khorana, *Proc. Natl. Acad. Sci. USA* **2002**, *99*, 13419 – 13424.
[42] R. Langen, K. Cai, C. Altenbach, H. Gobind Khorana, W. L. Hubbell, *Biochemistry* **1999**, *38*, 7918 – 7924.
[43] K. Werner, I. Lehner, H. K. Dhiman, C. Richter, C. Glaubitz, H. Schwalbe, J. Klein-Seetharaman, H. G. Khorana, *J. Biomol. NMR* **2007**, *37*, 303 – 312.
[44] K. Werner, C. Richter, J. Klein-Seetharaman, H. Schwalbe, *J. Biomol. NMR* **2008**, *40*, 49 – 53.
[45] E. Getmanova, A. B. Patel, J. Klein-Seetharaman, M. C. Loewen, P. J. Reeves, N. Friedman, M. Sheves, S. O. Smith, H. G. Khorana, *Biochemistry* **2004**, *43*, 1126 – 1133.
[46] J. Klein-Seetharaman, P. J. Reeves, M. C. Loewen, E. V. Getmanova, J. Chung, H. Schwalbe, P. E. Wright, H. G. Khorana, *Proc. Natl. Acad. Sci. USA* **2002**, *99*, 3452 – 3457.
[47] J. Klein-Seetharaman, N. V. K. Yanamala, F. Javeed, P. J. Reeves, E. V. Getmanova, M. C. Loewen, H. Schwalbe, H. G. Khorana, *Proc. Natl. Acad. Sci. USA*, **2004**, *101*, 3409 – 3413.
[48] O. P. Ernst, F. J. Bartl, *ChemBioChem* **2002**, *3*, 968 – 974.
[49] I. H. M. Van Stokkum, D. S. Larsen, R. Van Grondelle, *Biochim. Biophys. Acta Bioenerg.* **2004**, *1657*, 82 – 104.
[50] C. Slavov, H. Hartmann, J. Wachtveitl, *Anal. Chem.* **2015**, *87*, 2328 – 2336.
[51] F. J. Bartl, R. Vogel, *Phys. Chem. Chem. Phys.* **2007**, *9*, 1648 – 1658.

Received: June 24, 2015
Revised: August 11, 2015
Published online: September 18, 2015

